BIOMOLECULES & THERAPEUTICS

Original Article
Biomol Ther 24(6), 595-603 (2016)

Pyrrole-Derivative of Chalcone, (*E*)-3-Phenyl-1-(2-Pyrrolyl)-2-Propenone, Inhibits Inflammatory Responses via Inhibition of Src, Syk, and TAK1 Kinase Activities

Sungjae Yang[1], Yong Kim[1], Deok Jeong[1], Jun Ho Kim[1], Sunggyu Kim[2], Young-Jin Son[3], Byong Chul Yoo[4], Eun Jeong Jeong[5], Tae Woong Kim[6,*], In-Sook Han Lee[5] and Jae Youl Cho[1,*]

[1]Department of Genetic Engineering, [2]Research and Business Foundation, Sungkyunkwan University, Suwon 16419,
[3]College of Pharmacy, Sunchon National University, Suncheon 57922,
[4]Colorectal Cancer Branch, Research Institute, National Cancer Center, Gyeonggi 10408,
Departments of [5]Science Education, [6]Biochemistry, Kangwon National University, Chuncheon 24341, Republic of Korea

Abstract

(*E*)-3-Phenyl-1-(2-pyrrolyl)-2-propenone (PPP) is a pyrrole derivative of chalcone, in which the B-ring of chalcone linked to β-carbon is replaced by pyrrole group. While pyrrole has been studied for possible Src inhibition activity, chalcone, especially the substituents on the B-ring, has shown pharmaceutical, anti-inflammatory, and anti-oxidant properties via inhibition of NF-κB activity. Our study is aimed to investigate whether this novel synthetic compound retains or enhances the pharmaceutically beneficial activities from the both structures. For this purpose, inflammatory responses of lipopolysaccharide (LPS)-treated RAW264.7 cells were analyzed. Nitric oxide (NO) production, inducible NO synthase (iNOS) and tumor necrosis factor-α (TNF-α) mRNA expression, and the intracellular inflammatory signaling cascade were measured. Interestingly, PPP strongly inhibited NO release in a dose-dependent manner. To further investigate this anti-inflammatory activity, we identified molecular pathways by immunoblot analyses of nuclear fractions and whole cell lysates prepared from LPS-stimulated RAW264.7 cells with or without PPP pretreatment. The nuclear levels of p50, c-Jun, and c-Fos were significantly inhibited when cells were exposed to PPP. Moreover, according to the luciferase reporter gene assay after cotransfection with either TRIF or MyD88 in HEK293 cells, NF-κB-mediated luciferase activity dose-dependently diminished. Additionally, it was confirmed that PPP dampens the upstream signaling cascade of NF-κB and AP-1 activation. Thus, PPP inhibited Syk, Src, and TAK1 activities induced by LPS or induced by overexpression of these genes. Therefore, our results suggest that PPP displays anti-inflammatory activity via inhibition of Syk, Src, and TAK1 activity, which may be developed as a novel anti-inflammatory drug.

Key Words: Pyrrole, Chalcone, Anti-inflammatory activity, Macrophages, NF-κB

INTRODUCTION

Inflammation is an immunological defense mechanism that restores homeostasis from afflicted tissues and organs invaded by foreign pathogens. The general mechanism of this process seems quite simple viral or bacterial peptides are recognized by dendritic cells, followed by macrophage recruitment to the site of infection (Yu *et al*., 2014). Nonetheless, this simple process is maintained and regulated by rather complex interplays between immune cells and intracellular inflammatory pathway-dependent feedback loops. Similar to other biological process, due to its complexity of regulation, inflammation is not bulletproof and can produce errors. Such errors can lead to uncontrolled inflammatory responses that can harm the body (Screaton *et al*., 2015). In fact, a prolonged incidence of inflammation has been linked to several diseases such as, cancer, diabetes, and obesity (Lumeng and Saltiel, 2011; Elinav *et al*., 2013). Recently, our knowledge of inflammation mediating molecules has expanded from cytokines released from immune cells to damage-associated molecular patterns

Open Access https://doi.org/10.4062/biomolther.2016.027

Received Feb 11, 2016 **Revised** Apr 2, 2016 **Accepted** Apr 21, 2016
Published Online Nov 1, 2016

***Corresponding Authors**
E-mail: tawkim@kangwon.ac.kr (Kim TW), jaecho@skku.edu (Cho JY)
Tel: +82-33-250-8515 (Kim TW), +82-31-290-7868 (Cho JY)
Fax: +82-33-250-8510 (Kim TW), +82-31-290-7870 (Cho JY)

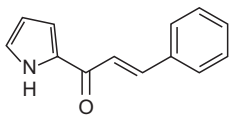

Fig. 1. Chemical structure of *(E)*-3-phenyl-1-(2-pyrrolyl)-2-propenone (PPP).

(DAMPs) such as heat-shock proteins, DNA, RNA, and high-mobility group box-1 (HMGB-1), which are largely connected to sepsis (Rittirsch *et al*., 2008). Hence, many institutional and pharmaceutical laboratories are focusing on not only on inflammatory pathway investigations but on finding substances that negatively modulate overly uncontrolled inflammatory responses, as well.

In laboratories, either lipopolysaccharide (LPS) or lipoteichoic acid are used to mimic gram-negative bacterial infection in *in vitro* systems using mouse-derived RAW264.7or human-derived THP-1 cell lines. When the cluster of differentiation-14 (CD-14) receptor is stimulated by LPS, it then delivers LPS to toll-like receptor 4(TLR4) and activates it (Chow *et al*., 1999). Upon its activation, TLR4 recruits myeloid differentiation primary-response protein-88 (MyD88) adaptor family members, including MyD88, toll-interleukin 1 receptor (TIR) domain containing adaptor protein (TIRAP), Toll/interleukin-1 (IL)-1 domain-containing adaptor inducing IFN-β (TRIF), and TRIF-related adaptor molecule (TRAM). MyD88 adaptor proteins link to TLR4 with IL-1 receptor associated kinase 1 (IRAK1) and IRAK4 followed by IRAK1 phosphorylation. Finally, TRAF6associates with IRAK1 to complete the complex (O'Neill, 2002). When this p-IRAK1-TRAF6 complex dissociates itself from adaptor proteins, it phosphorylates and forms a complex with TAK1 and TAB2. Phosphorylation of TAK1 and TAB2 results in ubiquitylation of TRAF6 leading to activation of TAK1 (Ajibade *et al*., 2013). Activated TAK1 interacts with the evolutionarily conserved signaling intermediate in toll pathway (ECSIT) protein to initiate NF-κB and AP-1 signaling cascades, through phosphorylation of IKK and MKKs, respectively (Akira and Takeda, 2004). Alternatively, MyD88 adaptor proteins are linked to Syk and Src kinase activation, which leads to TAK1-independent activation of NF-κB through p85 and AKT phosphorylation (Yang *et al*., 2012).

Previously, to develop novel anti-inflammatory drugs, our group has synthesized pyrrole derivatives of chalcone (Lee *et al*., 2013). It was previously reported that pyrrole may have ability to inhibit Src kinase activity, whereas chalcone has shown anti-oxidant, anti-inflammatory, anti-microbacterial, and anti-malarial activities (Lee *et al*., 2006; Dincer *et al*., 2013). In this study, one of them, *(E)*-3-phenyl-1-(2-pyrrolyl)-2-propenone (PPP) (Fig. 1) was selected and its anti-inflammatory activity was demonstrated by analyzing *in vitro* inflammatory responses of RAW264.7 cells stimulated by LPS. Finally, we evaluated the inhibitory mechanism of PPP in the context of the CD14 signaling cascade described above. The corresponding transcription factors regulating inflammatory responses were identified in PPP-treated cells.

MATRIALS AND METHODS

Materials

Polyethylenimine (PEI), PP2, piceatannol (Picea), 3-(4,5-dimethylthiazol-2-yl)-2,5-diphenyltetrazolium bromide (a tetrazole) (MTT), N_ω-nitro-L-arginine methyl ester (L-NAME), and lipopolysaccharide (LPS, *E. coli* 0111:B4) were purchased from Sigma Chemical Co. (St. Louis, MO, USA). Fetal bovine serum (FBS) and RPMI1640 were obtained from GIBCO (Grand Island, NY, USA). Dulbecco's modified Eagle's medium (DMEM) was obtained from Thermo Fisher Scientific Inc. (Waltham, MA, USA). RAW264.7 and HEK293 cells were purchased from ATCC (Rockville, MD, USA). All other chemicals used in this study were of analytical grade from Sigma Chemical Company. Phospho-specific or total-protein antibodies recognizing p65, p50, inhibitor of κBα (IκBα), Src, spleen tyrosine kinase (Syk), TAK1, c-Jun, c-Fos, ERK, JNK, c-Raf, IRAK1, MEK1/2, MKK4, Myc, HA, lamin A/C, and β-actin were obtained from Cell Signaling Technology (Beverly, MA, USA).

Preparation of *(E)*-3-phenyl-1-(2-pyrrolyl)-2-propenone

PPP was prepared, according to previously (Lee *et al*., 2013). Briefly, 2-Acetylpyrrole (0.83 g, 7.6 mmole) and benzaldehyde (0.81 g, 7.6 mmole) were added to an ice-cold solution of 2 M-NaOH (5 ml) and ethanol (7 ml). The resulting solution was gradually brought to room temperature and stirred for 5 h, followed by heating at 40°C for 30 min. The solution was neutralized with 1 M-HCl aqueous solution to pH 8-9 and then the resulting precipitate was collected and recrystallized from ethanol. The yield of the purified product was 77% and mp was 200°C.

Expression vectors and DNA transfection

DNA constructs with MyD88, TRIF, AP-1-Luc, and NF-κB-Luc were used, as reported previously (Yang *et al*., 2008; Byeon *et al*., 2013). All constructs were confirmed by automated DNA sequencing. Expression vectors were transfected in HEK293 cells by the PEI method in 12-well plates (1×10^6 cells/ml), as reported previously (Baek *et al*., 2015; Jeon *et al*., 2015). After 24 h, the transfected cells were treated with PPP for additional 24 h before termination.

Cell culture and drug preparation

RAW264.7 cells were cultured in RPMI1640 with 10% heat-inactivated FBS and 1% penicillin/streptomycin at 37°C in 5% CO_2. HEK293 cells were maintained in DMEM media supplemented with 5% heat-inactivated FBS and 1% penicillin/streptomycin at 37°C in 5% CO_2. The stock solutions of PPP for the *in vitro* experiments were prepared in dimethylsulfoxide (DMSO).

Determination of nitric oxide (NO) production

After pre-incubation of RAW264.7 cells (1×10^6 cells/ml) for 18 h, PPP, L-NAME, PP2, or piceatannol (Picea) were added to the cells for 30 min. After that, the cells were treated with LPS (1 μg/ml) for 24 h. The inhibitory effects of these compounds on the production of NO were determined by analyzing NO levels using Griess reagents (Lee *et al*., 2014c).

Cell viability test

The cytotoxic effects of PPP (0 to 100 μM) were evaluated using a conventional MTT assay, as previously reported (Pau-

wels *et al*., 1988; Lee *et al*., 2014a). For the final 3 h of culture, 10 μl of MTT solution (10 mg/ml in phosphate-buffered saline, pH 7.4) were added to each well. Reactions were stopped by the addition of 15% SDS into each well to solubilize the formazan. The absorbance at 570 nm ($OD_{570-630}$) was measured using a Spectramax 250 microplate reader (BioTex, Bad Friedrichshall, Germany).

mRNA analysis through semi-quantitative reverse transcriptase (RT)-polymerase chain reaction (PCR)

To evaluate cytokine mRNA expression levels, RAW264.7 cells pre-treated with PPP (0-100 μM) for 30 min were incubated with LPS (1 μg/ml) for 6 h. Total RNA was isolated using TRIzol Reagent (GIBCO), according to the manufacturer's instructions and stored at -70°C until further use. Semiquantitative RT reactions were conducted as previously reported (Lee *et al*., 2014b). The primers (Bioneer, Seoul, Republic of Korea) used in these experiments are the same as previously published paper (Kim *et al*., 2016).

Luciferase reporter gene activity assay

HEK293 cells (1×10^6 cells/ml) were transfected with 1 μg plasmid containing NF-κB-Luc or AP-1-Luc along with β-galactosidase using the PEI method in a 24-well plate, according to the manufacturer's protocol. The cells were used for experiments 24 h after transfection. Luciferase assays were performed using the Luciferase Assay System (Promega, Madison, WI, USA), as reported previously.

Preparation of cell lysates and nuclear fractions for immunoblot analysis

RAW264.7 or HEK293 cells (5×10^6 cells/ml) were washed three times in cold PBS and lysed in lysis buffer as reported previously (Kim *et al*., 2014a). Nuclear lysates were prepared using a three-step procedure (Byeon *et al*., 2008). After treatment, the cells were collected with a rubber policeman, washed with 1×PBS, and lysed in 500 μl of lysis buffer on ice for 4 min. During the second step, the pellet (the nuclear fraction) was washed once with wash buffer without Nonidet P-40. During the final step, the nuclei were resuspended in an extraction buffer consisting of the lysis buffer plus 500 mM KCl and 10% glycerol. The nuclei/extraction buffer mixture was frozen at -80°C then thawed on ice and centrifuged at 14,000 rpm for 5 min. The supernatant was collected as the nuclear extract. Whole-cell or nuclear lysates were then analyzed by a conventional immunoblot method (Yang *et al*., 2014). The total and phosphorylated levels of p65, p50, IκBα, Src, Syk, TAK1, c-Jun, c-Fos, ERK, JNK, c-Raf, IRAK1, MEK1/2, MKK4, Myc, HA, lamin A/C, and β-actin were visualized using an ECL system (Amersham, Little Chalfont, Buckinghamshire, UK), as reported previously (Kim *et al*., 2014b).

Statistical analyses

All of the data presented in this paper are expressed as means ± SD. For statistical comparisons, results were analyzed using either ANOVA/Scheffe's *post-hoc* test or the Kruskal-Wallis/Mann-Whitney test. A *p*-value <0.05 was considered to be statistically significant. All statistical tests were carried out using the computer program, SPSS (SPSS Inc., Chicago, IL, USA).

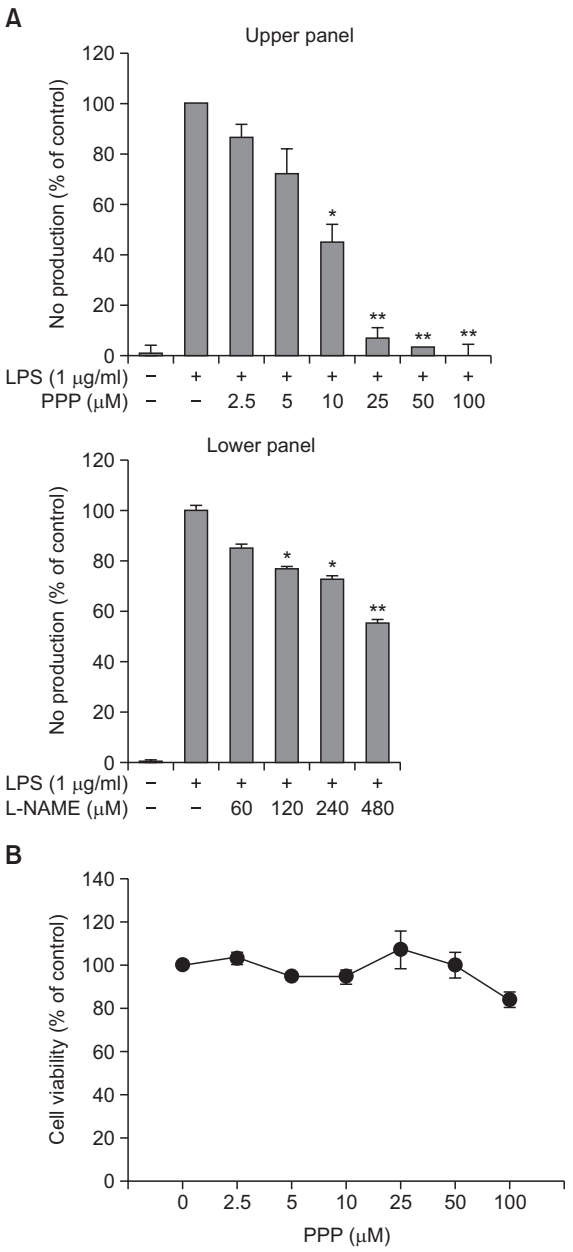

Fig. 2. Effect of PPP on the production of NO from LPS-stimulated RAW264.7 and on the viability of RAW264.7 cells. (A) RAW264.7 cells were plated on 96-well microplate (1×10^6 cells/ml), and were stimulated with LPS (1 μg/ml) in the absence or presence of PPP (2.5 to 100 μM) or L-NAME (60 to 480 μM) for 24 h. The NO levels in the supernatants were determined using Griess assay. (B) RAW264.7 cells (1×10^6 cells/ml) were treated with PPP (0 to 100 μM) for 24 h followed by MTT assay to determine its cytotoxicity. All data are expressed as the mean ± SD of experiments, which were performed with six samples. **p*<0.05 and ***p*<0.01 compared to normal or control groups.

RESULTS

Effect of PPP on the production of NO from LPS-stimulated RAW264.7 cells

RAW264.7 cells were pretreated with a wide range of PPP

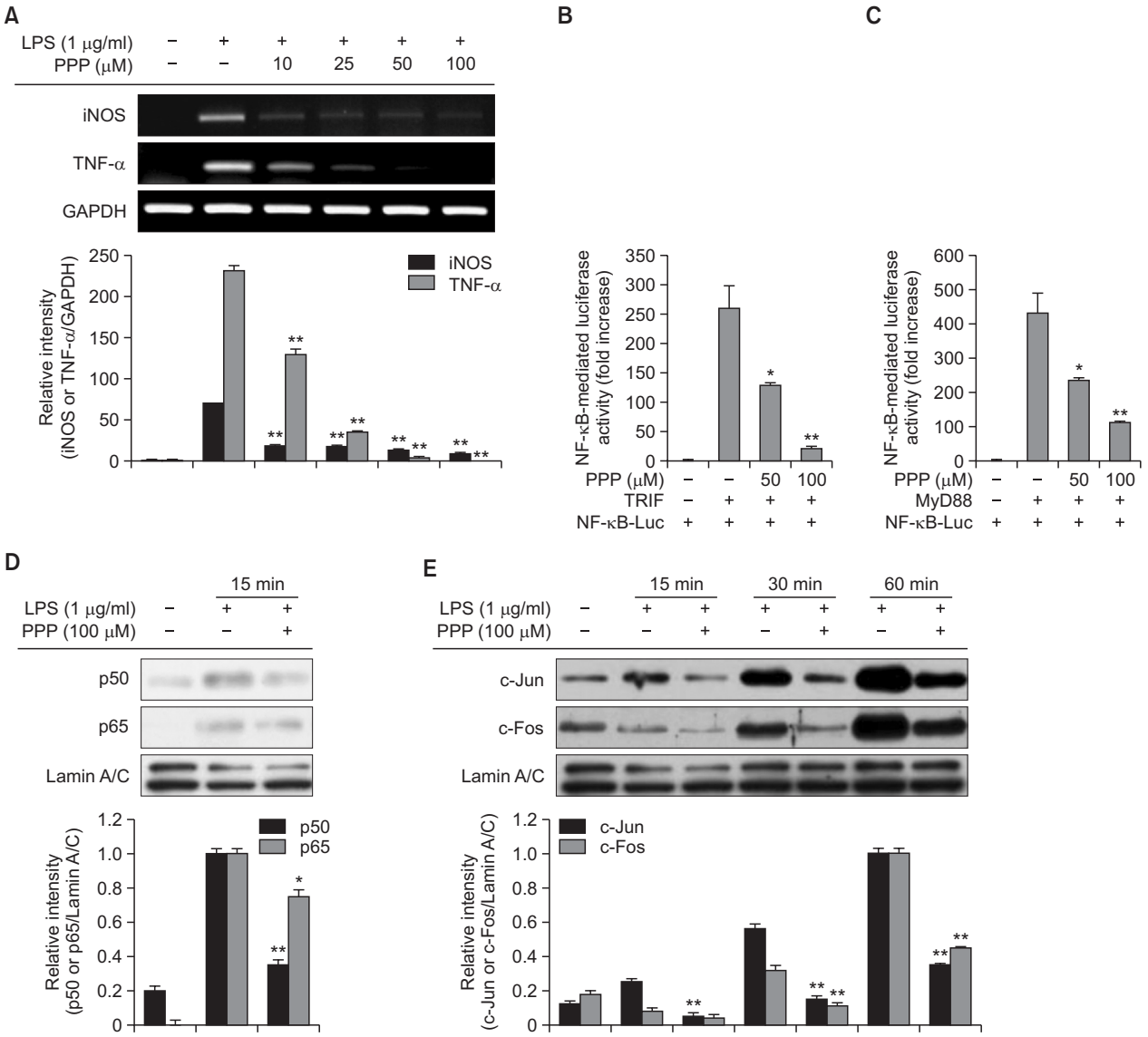

Fig. 3. Effect of PPP on the expression of inflammatory genes and transcriptional activation of inflammatory responses. (A) RAW264.7 cells were stimulated with LPS (1 μg/ml) in the absence or presence of incremental concentrations of PPP (10 to 100 μM) followed by mRNA isolation at 6 h after LPS treatment. Both iNOS and TNF-α mRNA levels were determined by using semi-quantitative RT-PCR. (B, C) HEK293 cells were co-transfected with NF-κB-Luc plasmid construct and β-gals in the presence or absence of TRIF or MyD88 followed by PPP (50 or 100 μM) treatment for 24 h. Luciferase activities were measured using a luminometer. (D, E) The nuclear levels of p65, p50, c-Jun, and c-Fos in LPS (1 μg/ml)-stimulated RAW264.7 cells in the presence or absence of PPP (100 μM) were detected by immunoblot analysis. Data are expressed as the mean ± SD of experiments, which were performed with six samples. Relative intensity was calculated using total levels by the DNR Bio-imaging system. **p*<0.05 and ***p*<0.01 compared to normal or control groups.

concentrations (0 to 100 μM) prior to LPS stimulation. Next, NO levels were analyzed using the Griess assay. The NO levels dose-dependently lowered as PPP concentrations increased (Fig. 2A, upper panel). Cytotoxic activity of the PPP was carried out to insure that the reduction of NO production was not simply due to reduced number of viable macrophages available under higher concentrations of PPP (Fig. 2B). The results from these experiments suggest that PPP effectively lowers NO production without non-specific cytotoxicity affecting the RAW264.7 macrophages. Meanwhile, standard compound, L-NAME, inhibited NO production in a dose-dependent manner (Fig. 2A, lower panel).

Effect of PPP on the transcriptional activation of inflammatory responses

The mRNA expression levels of iNOS and TNF-α were assayed using semi-quantitative RT-PCR to investigate how PPP treatment lowers NO production. The mRNA expression levels of iNOS are directly responsible for NO generation. The mRNA expression levels of TNF-α and iNOS are upregulated by active NF-κB pathways. The pattern shown in Fig. 2A left panel shows that the mRNA expression levels of both iNOS and TNF-α were reduced dose-dependently (Fig. 3A). In addition, the luciferase reporter gene assays determined whether the effects of PPP stimulation were derived from the lowered

transcriptional activity of NF-κB. HEK293 cells overexpressing TRIF or MyD88 adaptor molecules were co-transfected with NF-κB-Luc reporter genes followed by six h of incubation in the absence or presence of PPP (50 or 100 μM). Without PPP, both TRIF and MyD88 overexpression increased the transcriptional activity of NF-κB more than 250 and 400 folds, respectively. However, the increased activity of NF-κB was decreased by half with 50 μM of PPP and reduced to baseline with 100 μM of PPP (Fig. 3B, 3C). The nuclear levels of the NF-κB transcriptional factor subunits, p65 and p50, were determined in LPS-stimulated RAW264.7 cells with or without PPP (100 μM). The reduced nuclear level of p50 in the presence of PPP, shown in Fig. 3D, suggests that the compound may block nuclear translocation of NF-κB. Nonetheless, the nuclear level of p65 was not as conspicuous, implying that the drastic suppressive activity of the compound may derive from other signaling pathways. To test this hypothesis, we expanded the experimental design to determine the levels of other transcriptional factors, such as c-Jun and c-Fos (Fig. 3E). Surprisingly, PPP treatment dramatically inhibited nuclear translocation of both proteins at 15, 30, and 60 min after LPS stimulation in RAW264.7 cells, suggesting that the target of PPP could be early upstream in the CD14 signaling cascade, where it can affect both NF-κB and AP-1 signaling cascades.

Effect of PPP on the upstream signaling cascade for NF-κB activation

Phosphorylation and nuclear translocation of p65/p50 dimers are mediated by cytosolic degradation of IκBα (Brown *et al*., 1993). However, the mechanism leading to degradation of IκBα involves complicate intracellular signaling pathways under LPS-stimulated macrophages. Syk and Src kinases are also found to be involved in this mechanism and are responsible for their early activation (Yang *et al*., 2012). Whole cell lysate immunoblot analysis exhibited that LPS-induced IκBα phosphorylation at 5, 15, and 30 min were inhibited by the presence of PPP (Fig. 4A). In accordance with blockade of IκBα degradation, phosphorylation levels of both Syk and Src were inhibited in early time (Fig. 4B). These results suggest that the anti-inflammatory activity of PPP may come from inhibition of Syk and Src kinase activity.

Effect of PPP on the autophosphorylation of Src and Syk in the Src- or Syk-transfected HEK293 cells

The phosphorylated Src and Syk under LPS-stimulated RAW264.7 cells (Byeon *et al*., 2012) were inhibited by PPP (Fig. 4B). Therefore, to further determine whether PPP is able to directly inhibit the autophosphorylation of Syk or Src, overexpression of these enzymes in HEK293 cells was employed. In fact, overexpression of Src and Syk markedly increased the autophosphorylation of these enzymes (Fig. 5A, 5B). As we expect, PPP strongly dose-dependently diminished their autophosphorylation levels (Fig. 5A, 5B). Phosphorylation levels of both kinases were inhibited by PPP treatment. Meanwhile, standard Src and Syk inhibitors PP2 and piceatannol exhibited suppression of NO release (Fig. 5C), indicating that NO production could be positively managed by these enzymes.

Effect of PPP on the upstream signaling cascade for AP-1 activation

As shown in Fig. 3E, it was found that PPP is able to suppress the nuclear translocation of AP-1 (c-Jun and c-Fos).

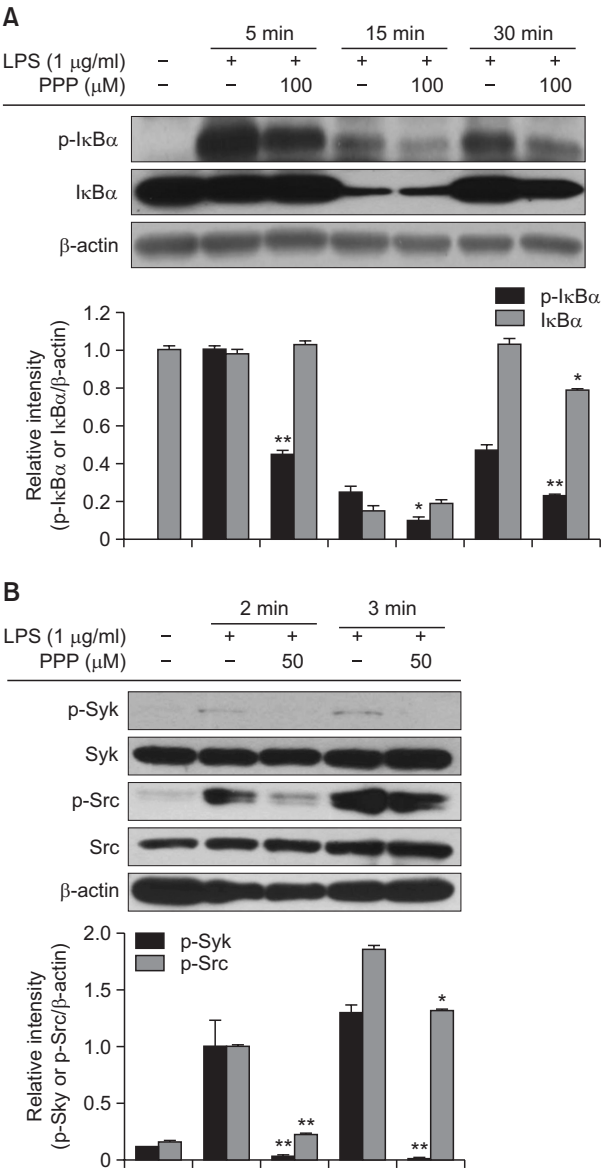

Fig. 4. Effect of PPP on the upstream signaling cascade for NF-κB activation in LPS-stimulated RAW264.7 cells. (A, B) RAW264.7 cells were incubated with the absence or presence of PPP (100 μM) were stimulated with LPS (1 μg/ml) for 2, 3, 5, 15, or 30 min. The total and phospho-protein levels of IκBα, Syk, and Src were determined by immunoblot analysis. Relative intensity was calculated using total levels by the DNR Bio-imaging system. *p<0.05 and **p<0.01 compared with controls.

Therefore, we next examined which protein regulating AP-1 translocation is targeted by PPP. Interestingly, the phosphorylation levels of JNK and ERK were also found to be inhibited by this compound (Fig. 6A). Similarly, the phosphorylation of upstream enzymes (MEK1/2, MKK4, and TAK1) contributing to the activation of JNK and ERK was also remarkably suppressed by PPP at 2 and 3 min, while degradation of IRAK1 and the phosphorylation of c-Raf were not blocked (Fig. 6B). Since TAK1 is a member of serine/threonine kinase family to activate AP-1 transcription factor by autophosphorylation and forming complex with TRAF6, we employed overexpression

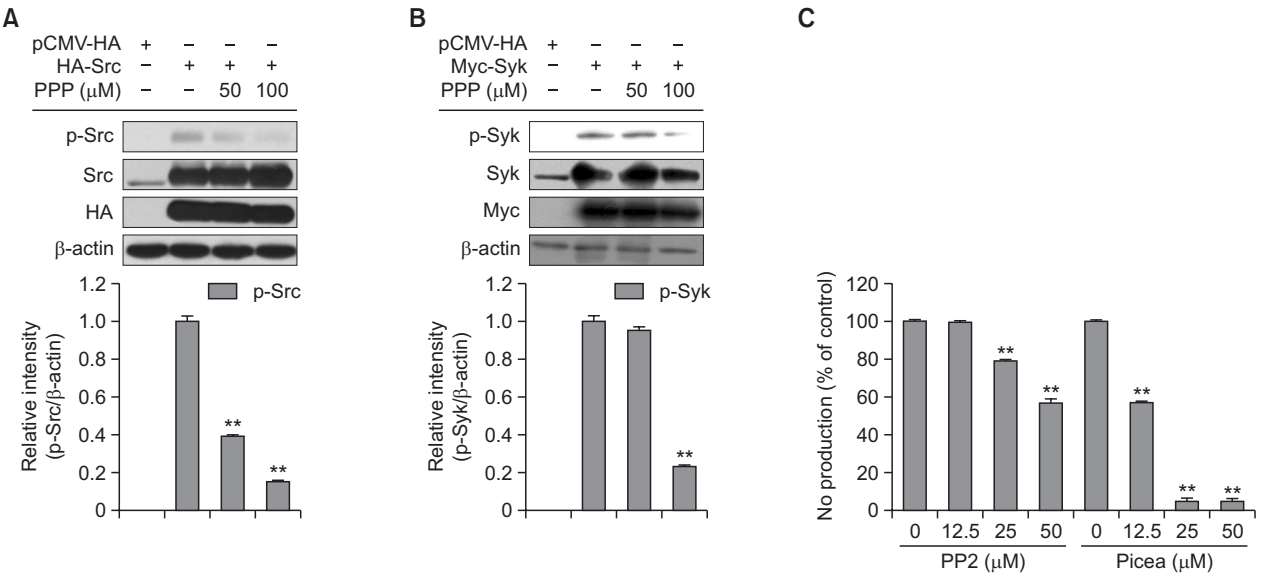

Fig. 5. Effect of PPP on the autophosphorylation of Src and Syk in the Src-or Syk-transfected HEK293 cells. (A, B) Inhibitory activity of PPP (50 and 100 μM) on the autophosphorylation of Src (A) or Syk (B) in the Src-or Syk-transfected HEK293 cells measured by immunoblot analysis. (C) RAW264.7 cells were plated on 96-well microplate (1×10^6 cells/ml), and were stimulated with LPS (1 μg/ml) in the absence or presence of PP2 (12.5, 25, and 50 μM) or Picea (12.5, 25, and 50 μM) for 24 h. The NO levels in the supernatants were determined using Griess assay. Relative intensity was calculated using total levels by the DNR Bio-imaging system. ***p*<0.01 compared with controls.

strategy with TAK1 gene. As we expected, TAK1 overexpression enhanced the level of TAK1 phosphorylation (Fig. 6C). Intriguingly, PPP (100 μM) clearly suppressed the TAK1 phosphorylation (Fig. 6C), implying that there is a possibility that PPP might block the autophosphorylation of TAK1.

DISCUSSION

Our synthetic compound, PPP, has shown its anti-inflammatory activities by suppression of both NF-κB and AP-1 pathways without affecting cell viability. Less than 10 μM of PPP is the half-maximal inhibitory concentration (IC_{50}) necessary to induce NO production in LPS-stimulated RAW264.7 cells (Fig. 2A). The major enzyme responsible for generation of NO under LPS stimulation, iNOS, was found to be significantly downregulated by PPP treatment (Fig. 3A). Since both iNOS and TNF-α were downregulated at the transcriptional level, their transcriptional factor, NF-κB, was assayed using nuclear fractionation and immunoblot analysis. The nuclear protein level of p50 was reduced in the PPP-treated groups (Fig. 3D), indicating the compound may interrupt the nuclear translocation of p50. These phenomena were confirmed using a luciferase reporter gene construct where dampened NF-κB transcriptional factor activity was observed in both TRIF- and MyD88-overexpressed HEK293 cells in a dose-dependent manner (Fig. 3B, 3C). The nuclear translocation of p65/p50 nuclear is regulated by IκBα degradation leaving p65/p50 NF-κB subunits to be released into the nucleus (Brown *et al*., 1993). Meanwhile, immunoblot analysis (Fig. 4A) revealed that PPP treatment is able to downregulate LPS-induced phosphorylation of IκBα in early times (5, 15, and 30 min). In addition, PPP prevented autophosphorylation of protein kinases responsible for early activation of macrophages and NF-κB signal transduction, such as Syk and Src (Fig. 4B, 5A, 5B). Based on our study, the mechanism of action of PPP in amelioration of the inflammatory response may be due to blockade of LPS-induced phosphorylation of Syk and Src, leading to dampened NF-κB signaling cascades. Although the nuclear level of p50 was reduced by PPP treatment, the p65 subunit of NF-κB was not affected by the PPP. Hence, it seems plausible to speculate that the anti-inflammatory properties of PPP may derive from blocking other signaling cascades. To confirm this hypothesis, the protein levels of the AP-1 subunits, c-Jun and c-Fos within nucleus, were also assayed using nuclear fractionation and immunoblot analysis. Surprisingly, both subunits were significantly diminished in the PPP-treated groups, supporting our hypothesis, that PPP also negatively affects AP-1 pathways (Fig. 3E). Similar to the approach employed for NF-κB transcription factors, the upstream cascades of AP-1 were also investigated. Previously, it was discovered that autophosphorylation of TAK1 occurs at serine (Ser)-192 in its kinase activation loop (Kishimoto *et al*., 2000).

When treated with PPP, TAK1 overexpression in HEK293 cells showed depressed TAK1 Ser-192 phosphorylation (Fig. 6C), indicating that the downregulated AP-1 signal may be derived from this step. The inhibition of phospho-TAK1 by PPP was repeated in whole cell lysate prepared from LPS-stimulated RAW264.7 cells, whereas the total protein level of IRAK1, a MyD88 adaptor protein recruited after TLR4 activation (Nahid *et al*., 2011), remained the same regardless of PPP treatment (Fig. 6B). While it is already known that IRAK1 degradation is necessary for the formation of the TRAF6-TAK1 complex to be dissociated from the MyD88-adaptor complex and localized in cytosol for further signal transduction, it does not mediate TAK1 phosphorylation (Akira and Takeda, 2004). Hence, this evidence suggests that PPP is involved in not inhibition of TRAF6-TAK1 complex translocation, but significant impairment of TAK1 kinase activity. Supportively, the decreased TAK1 autophosphorylation level at Ser-192 in the PPP-treated

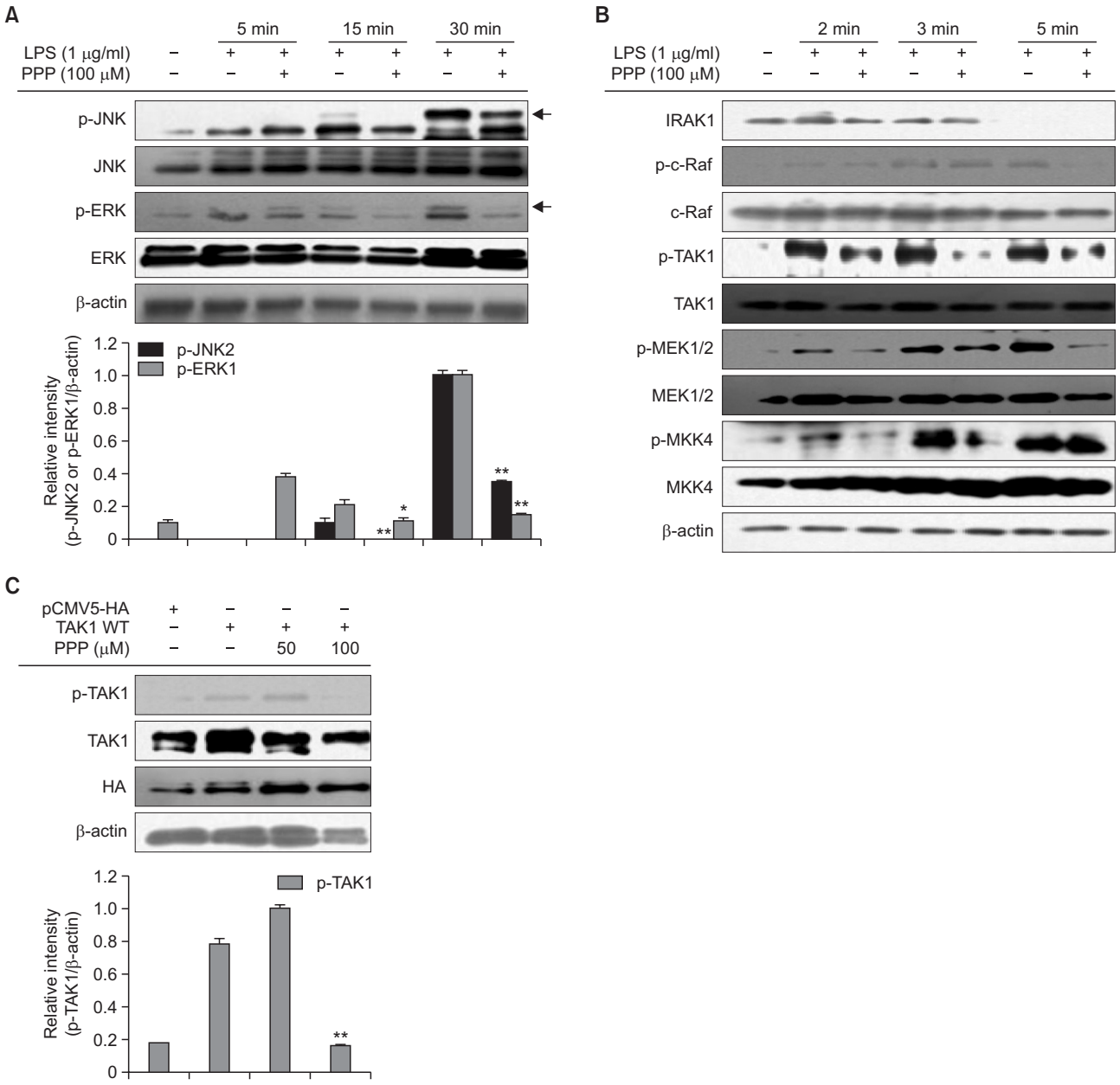

Fig. 6. Effect of PPP on the suppression of AP-1 upstream cascades. (A, B, and C) The phosphorylation and degradation levels of JNK, ERK, MKK4, MEK1/2, TAK1, c-Raf, and IRAK1 in LPS-treated RAW264.7 cells and the autophosphorylation pattern of TAK1 in TAK1-overexpressed cells in the presence or absence of PPP (50 and 100 μM) were measured by immunoblot analysis. Relative intensity was calculated using total levels by the DNR Bio-imaging system. *p<0.05, **p<0.01 compared with controls.

groups seems to lower phosphorylation ratios of MAPK components, MEK1/2 and MKK4 (Fig. 6B). Consequently, reduced activation levels of MAPKs resulted in inhibition of ERK and JNK phosphorylation at 15 and 30 min after PPP treatment (Fig. 6A). Phosphorylated ERK and JNK directly phosphorylate and induce nuclear translocation of the AP-1 subunits, c-Jun and c-Fos (Cho *et al*., 2014). Therefore, TAK1-linked downregulation of ERK and JNK pathways under PPP exposure (Fig. 3E) could contribute to its AP-1 suppressive activity.

Although, NF-κB and AP-1 pathways regulate a vast range of genes that encode for pro-inflammatory cytokines and mediators such as IL-1β, prostaglandins (PGE_2), and matrix metalloproteinase 7 (MMP7) (Tran *et al*., 2014; Shao *et al*., 2015), there are still many aspects of PPP properties that have not yet been investigated. We believe that the PPP treatment will have beneficial effects on various *in vivo* diseases models such as gastritis, hepatitis, colitis, arthritis, and pancreatitis. Nonetheless, in order to fully understand and benefit from PPP's anti-inflammatory properties, discovery of the compound-protein binding site on target proteins is required. Moreover, as in studies performed on structure-activity relationships of the B-ring in chalcone, our future goals include the analysis of PPP's anti-inflammatory activity by manipulating its functional group in the pyrrole ring. Hence, by additional

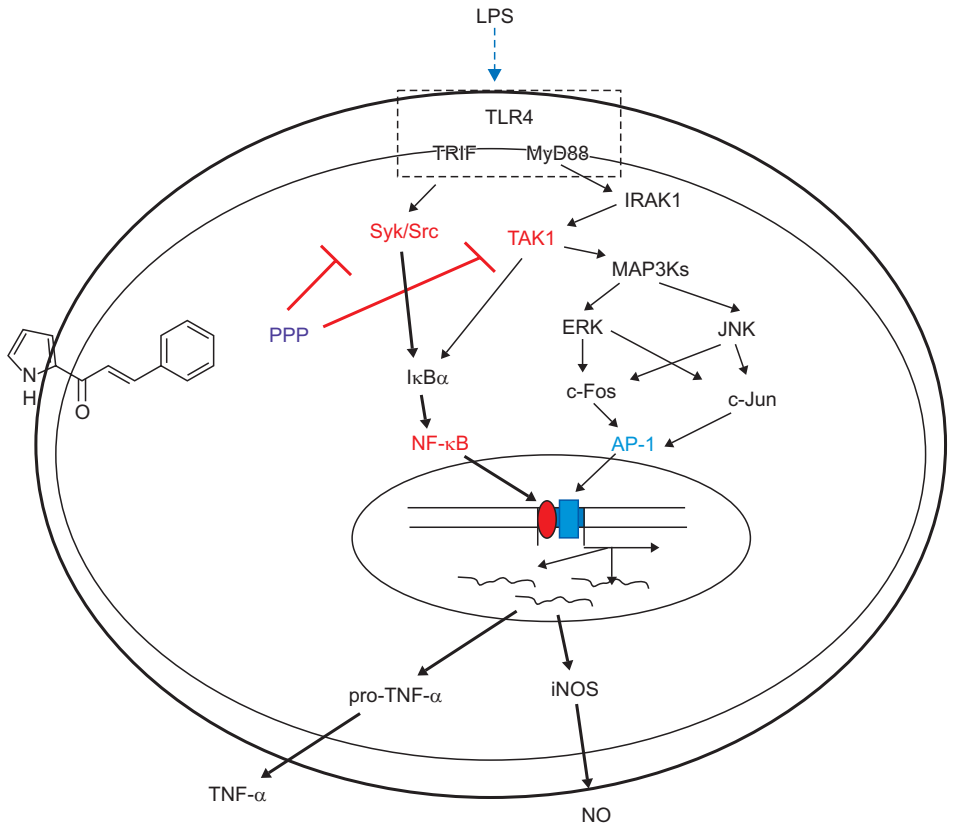

Fig. 7. Putative anti-inflammatory pathway of PPP in LPS-treated macrophages.

molecular and *in vivo* pharmacological studies, the drug value of our chalcone pyrrole-derivative compound may be further examined in the future.

In summary, we found that PPP suppresses the release of NO and reduces the mRNA expression of inflammatory genes (iNOS and TNF-α). Moreover, this compound inhibited a series of elements in key inflammatory signaling cascades such as the phosphorylation of Src, Syk, and TAK1, as well as the subsequent translocation of p50/NF-κB and AP-1 (summarized in Fig. 7). Since PPP exhibited strong anti-inflammatory effects, we propose that this compound can be further developed as a strong anti-inflammatory drug to treat various inflammatory symptoms. Therefore, additional pre-clinical studies are necessary.

DISCLAIMER

The authors alone are responsible for the content and writing of the paper.

CONFLICT OF INTEREST

The authors report no conflict of interests.

ACKNOWLEDGMENTS

This research was supported by a research grant from Kangwon National University (no. 120131232) and by the BK21 plus program through the National Research Foundation (NRF) funded by the Ministry of Education of Korea.

REFERENCES

Ajibade, A. A., Wang, H. Y. and Wang, R. F. (2013) Cell type-specific function of TAK1 in innate immune signaling. *Trends Immunol.* **34**, 307-316.

Akira, S. and Takeda, K. (2004) Toll-like receptor signalling. *Nat. Rev. Immunol.* **4**, 499-511.

Baek, K. S., Hong, Y. D., Kim, Y., Sung, N. Y., Yang, S., Lee, K. M., Park, J. Y., Park, J. S., Rho, H. S., Shin, S. S. and Cho, J. Y. (2015) Anti-inflammatory activity of AP-SF, a ginsenoside-enriched fraction, from Korean ginseng. *J. Ginseng Res.* **39**, 155-161.

Brown, K., Park, S., Kanno, T., Franzoso, G. and Siebenlist, U. (1993) Mutual regulation of the transcriptional activator NF-κB and its inhibitor, IκBα. *Proc. Natl. Acad. Sci. U.S.A.* **90**, 2532-2536.

Byeon, S. E., Yi, Y.-S., Oh, J., Yoo, B. C., Hong, S. and Cho, J. Y. (2012) The role of Src kinase in macrophage-mediated inflammatory responses. *Mediators Inflamm.* **2012**, 512926.

Byeon, S. E., Lee, Y. G., Kim, B. H., Shen, T., Lee, S. Y., Park, H. J., Park, S.-C., Rhee, M. H. and Cho, J. Y. (2008) Surfactin blocks NO production in lipopolysaccharide-activated macrophages by inhibiting NF-κB activation. *J. Microbiol. Biotechnol.* **18**, 1984-1989.

Byeon, S. E., Yu, T., Yang, Y., Lee, Y. G., Kim, J. H., Oh, J., Jeong, H. Y., Hong, S., Yoo, B. C., Cho, W. J., Hong, S. and Cho, J. Y. (2013)

Hydroquinone regulates hemeoxygenase-1 expression via modulation of Src kinase activity through thiolation of cysteine residues. *Free Radic. Biol. Med.* **57**, 105-118.

Cho, B. O., Ryu, H. W., So, Y., Lee, C. W., Jin, C. H., Yook, H. S., Jeong, Y. W., Park, J. C. and Jeong, I. Y. (2014) Anti-Inflammatory Effect of Mangostenone F in Lipopolysaccharide-Stimulated RAW264.7 Macrophages by Suppressing NF-κB and MAPK Activation. *Biomol. Ther. (Seoul)* **22**, 288-294.

Chow, J. C., Young, D. W., Golenbock, D. T., Christ, W. J. and Gusovsky, F. (1999) Toll-like receptor-4 mediates lipopolysaccharide-induced signal transduction. *J. Biol. Chem.* **274**, 10689-10692.

Dincer, S., Cetin, K. T., Onay-Besikci, A. and Ölgen, S. (2013) Synthesis, biological evaluation and docking studies of new pyrrolo [2, 3-d] pyrimidine derivatives as Src family-selective tyrosine kinase inhibitors. *J. Enzyme Inhib. Med. Chem.* **28**, 1080-1087.

Elinav, E., Nowarski, R., Thaiss, C. A., Hu, B., Jin, C. and Flavell, R. A. (2013) Inflammation-induced cancer: crosstalk between tumours, immune cells and microorganisms. *Nat. Rev. Cancer* **13**, 759-771.

Jeon, B. R., Kim, S. J., Hong, S. B., Park, H. J., Cho, J. Y. and Rhee, M. H. (2015) The inhibitory mechanism of crude saponin fraction from Korean Red Ginseng in collagen-induced platelet aggregation. *J. Ginseng Res.* **39**, 279-285.

Kim, K. H., Kim, T. S., Lee, J. G., Park, J. K., Yang, M., Kim, J. M., Jo, E. K. and Yuk, J. M. (2014a) Characterization of Proinflammatory Responses and Innate Signaling Activation in Macrophages Infected with Mycobacterium scrofulaceum. *Immune Netw.* **14**, 307-320.

Kim, M. Y., Yoo, B. C. and Cho, J. Y. (2014b) Ginsenoside-Rp1-induced apolipoprotein A-1 expression in the LoVo human colon cancer cell line. *J. Ginseng Res.* **38**, 251-255.

Kim, Y., Jeong, E. J., Han Lee, I. S., Kim, M. Y. and Cho, J. Y. (2016) *(E)*-3-(3-methoxyphenyl)-1-(2-pyrrolyl)-2-propenone displays suppression of inflammatory responses via inhibition of Src, Syk, and NF-κB. *Korean J. Physiol. Pharmacol.* **20**, 91-99.

Kishimoto, K., Matsumoto, K. and Ninomiya-Tsuji, J. (2000) TAK1 mitogen-activated protein kinase kinase kinase is activated by autophosphorylation within its activation loop. *J. Biol. Chem.* **275**, 7359-7364.

Lee, H. S., Lee, G. S., Kim, S. H., Kim, H. K., Suk, D. H. and Lee, D. S. (2014a) Anti-oxidizing effect of the dichloromethane and hexane fractions from Orostachys japonicus in LPS-stimulated RAW 264.7 cells via upregulation of Nrf2 expression and activation of MAPK signaling pathway. *BMB Rep.* **47**, 98-103.

Lee, I. S. H., Jeoung, E. J. and Lee, C. K. (2013) Synthesis and NMR Studies of *(E)*-1-Aryl-3-(2-pyrrolyl)-2-propenones and *(E)*-3-Aryl-1-(2-pyrrolyl)-2-propenones. *Bull. Korean Chem. Soc.* **34**, 936-942.

Lee, J.-H., Jung, H. S., Giang, P. M., Jin, X., Lee, S., Son, P. T., Lee, D., Hong, Y.-S., Lee, K. and Lee, J. J. (2006) Blockade of nuclear factor-κB signaling pathway and anti-inflammatory activity of cardamomin, a chalcone analog from Alpinia conchigera. *J. Pharmacol. Exp. Ther.* **316**, 271-278.

Lee, N., Jung, Y. S., Lee, H. Y., Kang, N., Park, Y. J., Hwang, J. S., Bahk, Y. Y., Koo, J. and Bae, Y. S. (2014b) Mouse neutrophils express functional umami taste receptor T1R1/T1R3. *BMB Rep.* **47**, 649-654.

Lee, Y. J., Han, J. Y., Lee, C. G., Heo, K., Park, S. I., Park, Y. S., Kim, J. S., Yang, K. M., Lee, K. J., Kim, T. H., Rhee, M. H. and Kim, S. D. (2014c) Korean Red Ginseng saponin fraction modulates radiation effects on lipopolysaccharide-stimulated nitric oxide production in RAW264.7 macrophage cells. *J. Ginseng Res.* **38**, 208-214.

Lumeng, C. N. and Saltiel, A. R. (2011) Inflammatory links between obesity and metabolic disease. *J. Clin. Invest.* **121**, 2111-2117.

Nahid, M. A., Satoh, M. and Chan, E. K. (2011) MicroRNA in TLR signaling and endotoxin tolerance. *Cell. Mol. Immunol.* **8**, 388-403.

O'Neill, L. A. (2002) Signal transduction pathways activated by the IL-1 receptor/toll-like receptor superfamily. *Curr. Top. Microbiol. Immunol.* **270**, 47-61.

Pauwels, R., Balzarini, J., Baba, M., Snoeck, R., Schols, D., Herdewijn, P., Desmyter, J. and De Clercq, E. (1988) Rapid and automated tetrazolium-based colorimetric assay for the detection of anti-HIV compounds. *J. Virol. Methods* **20**, 309-321.

Rittirsch, D., Flierl, M. A. and Ward, P. A. (2008) Harmful molecular mechanisms in sepsis. *Nat. Rev. Immunol.* **8**, 776-787.

Screaton, G., Mongkolsapaya, J., Yacoub, S. and Roberts, C. (2015) New insights into the immunopathology and control of dengue virus infection. *Nat. Rev. Immunol.* **15**, 745-759.

Shao, H. J., Lou, Z., Jeong, J. B., Kim, K. J., Lee, J. and Lee, S. H. (2015) Tolfenamic Acid Suppresses Inflammatory Stimuli-Mediated Activation of NF-κB Signaling. *Biomol. Ther. (Seoul)* **23**, 39-44.

Tran, V. G., Cho, H. R. and Kwon, B. (2014) IL-33 Priming Enhances Peritoneal Macrophage Activity in Response to Candida albicans. *Immune Netw.* **14**, 201-206.

Yang, K.-J., Shin, S., Piao, L., Shin, E., Li, Y., Park, K. A., Byun, H. S., Won, M., Hong, J., Kweon, G. R., Hur, G. M., Seok, J. H., Chun, T., Brazil, D. P., Hemmings, B. A. and Park, J. (2008) Regulation of 3-phosphoinositide-dependent protein kinase-1 (PDK1) by Src involves tyrosine phosphorylation of PDK1 and Src homology 2 domain binding. *J. Biol. Chem.* **283**, 1480-1491.

Yang, W. S., Lee, J., Kim, T. W., Kim, J. H., Lee, S., Rhee, M. H., Hong, S. and Cho, J. Y. (2012) Src/NF-κB-targeted inhibition of LPS-induced macrophage activation and dextran sodium sulphate-induced colitis by Archidendron clypearia methanol extract. *J. Ethnopharmacol.* **142**, 287-293.

Yang, Y., Yang, W. S., Yu, T., Yi, Y.-S., Park, J. G., Jeong, D., Kim, J. H., Oh, J. S., Yoon, K., Kim, J.-H. and Cho, J. Y. (2014) Novel anti-inflammatory function of NSC95397 by the suppression of multiple kinases. *Biochem. Pharmacol.* **88**, 201-215.

Yu, T., Li, Y. J., Bian, A. H., Zuo, H. B., Zhu, T. W., Ji, S. X., Kong, F., Yin de, Q., Wang, C. B., Wang, Z. F., Wang, H. Q., Yang, Y., Yoo, B. C. and Cho, J. Y. (2014) The regulatory role of activating transcription factor 2 in inflammation. *Mediators Inflamm.* **2014**, 950472.